https://doi.org/10.5194/egusphere-2026-2998
Preprint. Discussion started: 10 June 2026

Enhanced Carbon Sequestration in Alkaline Lakes through Recycled CO_2 Utilization by Diatoms

Dinggui Wu[1,2], Qingfeng Zhao[1], Siyu Huang[3], Yuxin He[1], Jinglu Wu[4], Yongge Sun[1]

[1]Organic Geochemistry Unit, School of Earth Sciences, Zhejiang University, Hangzhou 310027, China
[2]College of Oceanography, Hohai University, Nanjing210024, China
[3]College of Environment and Resources, Guangxi Normal University, Guilin 541004, China
[4]State Key Laboratory of Lake Science and Environment, Nanjing Institute of Geography and Limnology, Chinese Academy of Sciences (CAS), Nanjing 210008, China.

Correspondence to: Yongge Sun (ygsun@zju.edu.cn)

Abstract. Recycling of microbial respiration-derived CO_2(aq) plays a crucial role in regulating carbon sequestration and emissions in alkaline lakes, yet the extent to be assimilated by primary producers remains poorly constrained. In this study, a total of 35 surface sediments were collected across Lake Haixihai and organic molecular as well as carbon isotopic geochemical methods were employed to investigated the efficiency of diatom uptake of respiration-derived CO_2(aq). The results show that organic matter in surface sediments is dominated by aquatic macrophytes and terrigenous inputs, with minor contributions from algae and bacteria. The diatom-sourced C_{25} highly branched isoprenoids (HBIs) were detected in all sediments with $C_{25:2}$ HBI as the most abundant HBI. The $\delta^{13}C$ values of $C_{25:2}$ HBI strongly correlates with $\delta^{13}C_{org}$ (r = 0.946, p < 0.001) and the extent of microbial reworking as indicated by concentrations of $C_{30}\beta\beta$-hopane + hopenes and lignin-derived P/(V+S) ratios (r = -0.92 ~ -0.93, p < 0.001), suggesting that diatoms can substantially assimilate respiration-derived CO_2(aq). A two-endmember mixing model reveals that the respiration-derived CO_2(aq) utilized by diatoms accounts for an estimated 31% ± 8% of diatom carbon uptake. Comparisons across oceans, lakes, and wetlands show that inland waters sustain substantial recycling of respiration-derived CO_2(aq), which is efficiently assimilated by diatoms and reintegrated into the biological carbon pump. These findings suggest that lakes should not be recognized easily as conduits for terrestrial carbon loss. They are active systems in which biological re-fixation of respiration-derived CO_2(aq) can substantially enhance long-term carbon sequestration and mitigate CO_2 emissions.

1 Introduction

Lakes play a pivotal role in regional climate regulation and the global carbon cycle by receiving catchment inputs and transforming carbon through primary production, heterotrophic respiration, and carbon emission (Cole et al., 2007; Tranvik et al., 2009). The biological carbon pump is regarded as a key mechanism for stable carbon sink, as primary producers assimilate CO_2(aq) into organic matter that can subsequently be exported downward and buried in sediments (Liu, 2023). During this process, microbial reworking of organic matter in the water column and sediments produces respiration-derived

https://doi.org/10.5194/egusphere-2026-2998
Preprint. Discussion started: 10 June 2026

dissolved inorganic carbon (DIC), which can react with Ca^{2+} to form authigenic carbonates. This is considered another important pathway for reducing carbon emissions and enhancing carbon sequestration (Sun et al., 2019). However, whether this recycled DIC can also be reutilized by primary producers and return to the biological carbon pump remains ambiguous.

Diatoms are well known to dominate DIC uptake in lakes, particularly alkaline lakes, and facilitate particle export through their siliceous frustules, efficiently transferring newly fixed carbon from the water column to sediments, thus supporting carbon sequestration in alkaline lakes (Raven & Waite, 2004). They are also considered to be capable of utilizing respiration-derived DIC to support photosynthesis although direct evidence of diatoms assimilating recycled DIC is scarce (He et al., 2016). Compared with acidic lakes, alkaline lakes generally have larger DIC pools and stable diatom communities (Karst-Riddoch et al., 2005; Oduor & Schagerl, 2007; Duarte et al., 2008; Stenger-Kovács et al., 2014). This makes alkaline lakes an idea natural laboratory to examine whether recycled DIC can be substantially reused by primary producers (here diatom), and further regulate carbon sequestration and carbon emission within lake systems.

Stable carbon isotopes ($\delta^{13}C$) have provided potentials for assessing this hypothesis. Generally, microbial respiration produces ^{13}C-depleted DIC (Whiticar, 1999), whereas external inorganic carbon, mainly from carbonate weathering (0‰ ~ 2‰; Telmer & Veizer, 1999) and atmospheric exchange (-8‰; Dubois et al., 2010), is ^{13}C-enriched. Hence, respiration-derived carbon can strongly influence stable carbon isotopic compositions of DIC in lakes (*e.g.*, Striegl et al., 2001; Bade et al., 2004; Karlsson et al., 2007; Leigh McCallister & del Giorgio, 2008). Although carbonate dissolution and external DIC input often mask isotopic signals (Webb et al., 2016; Pietzsch, 2026), Sun et al. (2019) identified a key line of evidence for autogenic carbonate, showing that $\delta^{13}C$ values of sedimentary carbonate ($\delta^{13}C_{carb}$) respond sensitively to variations in $\delta^{13}C$ values of sedimentary organic matter ($\delta^{13}C_{org}$). Following this finding, the isotopic signature of carbon fixed by diatoms can act as a bridge to that of respiratory substrates, thus can serve as a potential proxy to trace the transfer of recycled CO_2(aq) into diatom production.

However, two main challenges exist in establishing an isotopic correlation between respired-derived DIC and diatom-sourced carbon. The first challenge is to identify sources of organic carbon (OC) because different OC sources exhibit distinct $\delta^{13}C$ compositions in the DIC released during microbial respiration (Bade et al., 2004; Karlsson et al., 2007; Sobek et al., 2009). Bulk geochemical indicators ($\delta^{13}C_{org}$, TOC/TN, $\delta^{15}N$) are only used to characterize the integrated properties of organic matter (Meyers & Ishiwatari, 1993). Source-specific biomarkers have been proved to be a powerful tool for constraining contributions of specific biogenic sources, such as diatoms, microorganisms, and aquatic macrophytes, as well as transformation processes (*e.g.*, biogenic activity, diagenetic alterations, etc.; Meyers & Ishiwatari, 1993; Hedges et al., 1997; Belt et al., 2000). The second challenge lies in direct determining diatom $\delta^{13}C$ in natural lakes due to mixed communities, small cell size, post-depositional degradation, and low separation efficiency. Although previous studies have measured carbon isotopes of isolated diatom biomass or siliceous frustules, sample purity and representativeness complicate the interpretation of isotopic data (Vuorio et al., 2006; Hurrell et al., 2011; Webb et al., 2016). As an alternative way, diatom-specific biomarkers and their carbon isotopes could be a potential proxy for this purpose. The C_{25} highly branched isoprenoids (C_{25} HBIs), produced by specific diatom groups (Rowland & Robson, 1990; Summons et al., 1993; Belt et al.,

https://doi.org/10.5194/egusphere-2026-2998
Preprint. Discussion started: 10 June 2026

2000), have been successfully applied to source determination in marine environments (e.g., Rowland & Robson, 1990; Summons et al., 1993; Belt et al., 2008; Belt et al., 2016; Kaiser et al., 2016) and are now being extended to lake systems (*e.g.*, Aichner et al., 2010; Zhang et al., 2018; Diefendorf et al., 2025). This is further supported by carbon isotopic compositions of individual C_{25} HBIs as they retain compound-specific $\delta^{13}C$ signatures that reflect the DIC assimilated during biosynthesis, while minimizing source-mixing issues (Belt et al., 2000; Kaiser et al., 2016). Therefore, C_{25} HBIs can serve as a practical tool for tracing the carbon sources utilized by diatoms via carbon isotope measurements.

In this study, Lake Haixihai, a small alpine alkaline lake in Yunnan province of southwest China, was selected to investigate whether recycled DIC can be reutilized significantly by primary producers (here diatom) and return to the biological carbon pump. By integrating bulk geochemical indicators of sedimentary organic matter with diatom-specific C_{25} HBIs and their compound-specific carbon isotopic compositions, this study aims to (i) determine the sources of sedimentary organic matter, (ii) identify the utilization of respiration-derived CO_2(aq) by diatoms, and (iii) quantify the efficiency of diatoms in utilizing recycled carbon. This study fills a gap in our understanding of internal carbon cycling within lake systems and offers new perspectives for evaluating carbon sequestration efficiency and carbon emission in different aquatic systems.

2 Sampling and experimental

2.1 Study area and sampling

Lake Haixihai (26°16′ ~ 26°31′N, 99°57′ ~ 99°59′E) is located in northwest Yunnan Province (Fig. 1a). It lies at an elevation of approximately 2,130 m and has a maximum water depth of 22 m. The lake extends in a northeast-southwest direction, with a length of approximately 3.7 km from north to south, a width of roughly 1.7 km from east to west, a total area of about 3 km^2, and a catchment area of around 23 km^2.

The surrounding catchment is predominantly composed of carbonate and silicate rocks, which formed a typical karst landscape and contributes to the alkaline nature of the lake (Wang et al., 2019; Lai et al., 2024). The lake water had a pH of 8.0 in March 2023. Surrounding vegetation is dominated by woody plants, with coniferous and broadleaf forests mainly distributed in the eastern and southern areas. The main algal groups include Dinoflagellata, Chlorophyta, and Diatomeae (Dong et al., 2019). Our field survey in March 2023 shows that aquatic plants are widely distributed, especially in nearshore areas of the north, west, and south (Fig. 1b). The dominant species include *Potamogeton perfoliatus*, *Vallisneria natans*, *Myriophyllum spicatum*, *Najas minor*, and *Utricularia*.

Lake Haixihai is primarily recharged by natural precipitation and surface runoff. It has a single outflow on the eastern side, and the discharge is regulated by an artificial control system (WABD, 2012), resulting in a weak hydrodynamic condition within the lake. This lake is oligotrophic, with high water transparency (Secchi disk depth ~8 m) and low phytoplankton biomass (*Chl. a* concentration ~2.0 ug L^{-1}; Wang et al., 2019). Diatom assemblages are dominated by planktonic species such as *Cyclotella ocellata*, *Fragilaria crotonensis*, *Cyclostephanos dubius*, and *C. comta*, accompanied by benthic diatoms like *Achnanthes minutissima*, *small Fragilaria spp.*, *Navicula spp.*, and *Nizschia spp* (Wang et al., 2019).

https://doi.org/10.5194/egusphere-2026-2998
Preprint. Discussion started: 10 June 2026

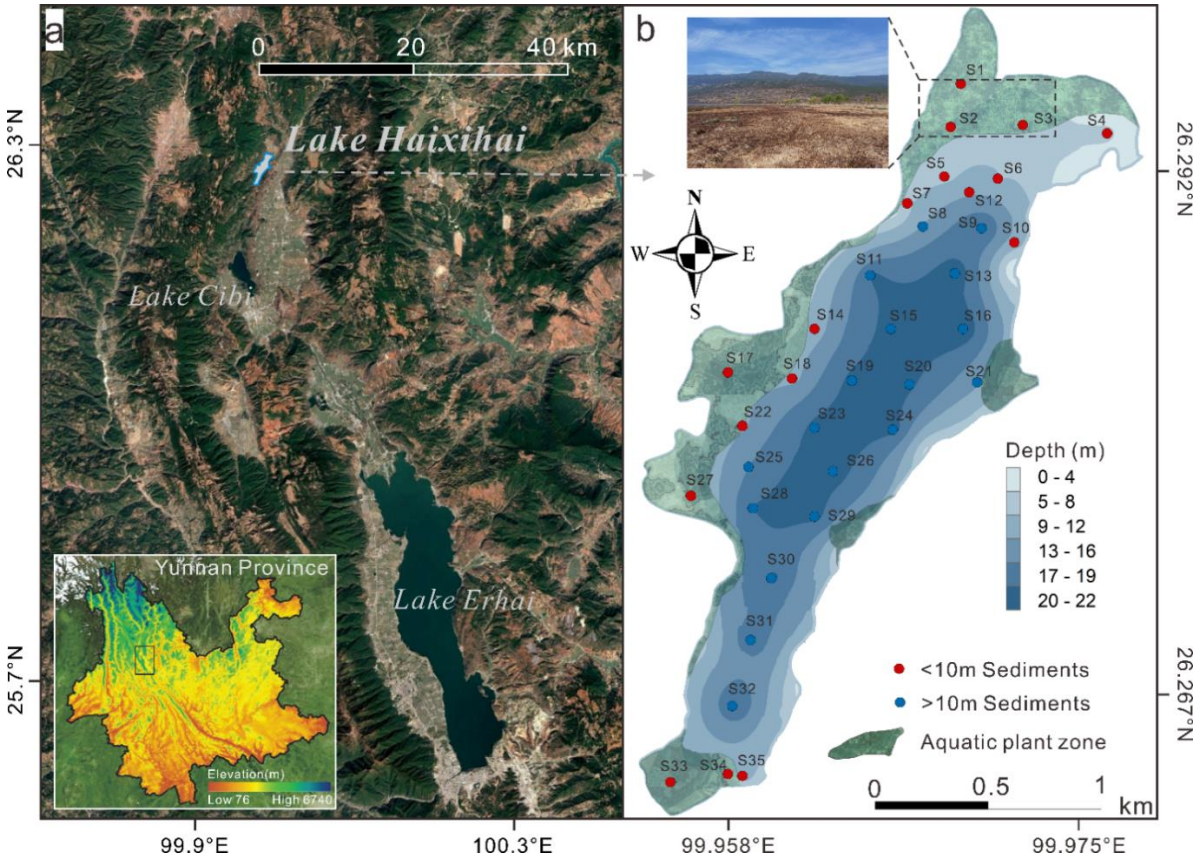

Figure 1: Map showing the geographic location of Lake Haixihai and sampling locations. a, Satellite map showing Lake Haixihai is located at the headwaters of Lake Erhai (the second largest freshwater lake in Yunnan Province). The inset in the lower left corner is an elevation map of Yunnan Province, and the black rectangular box shows the location of the satellite screenshot. Base map: Imagery © Google Earth 2024. The elevation data were obtained from the Yunnan Geographic Information Public Service Platform/Tianditu·Yunnan (https://yunnan.tianditu.gov.cn). b, Bathymetric map of Lake Haixihai showing the surface sediment sampling sites. The inset photo in the upper left corner of (b) shows the marsh wetland in the northern part of the lake.

A total of 35 sampling sites were designed (Fig. 1b), including 17 shallow water sites (< 10 m) and 18 deep water sites (> 10 m). Surface sediments representing the top 0 ~ 3 cm were collected using a Renberg® gravity corer in March 2023. Samples were immediately sealed in clean aluminum foil, placed in resealable bags, and stored in portable ice packs. Upon return to the laboratory, samples were stored at -20°C before analysis.

2.2 Bulk element and isotope analyses

Surface sediments were freeze-dried and ground to a fine powder (< 120 mesh). Carbonates were removed by treatment with 6N HCl, and the mass loss was used to calculate the percentage of $CaCO_3$ in sediments. Decarbonated samples were analyzed for total organic carbon (TOC) and stable carbon isotopes ($\delta^{13}C_{org}$). TOC and total nitrogen (TN) content were measured using a Euro Vector EA 3000 elemental analyzer. $\delta^{13}C_{org}$ was determined using a Thermo Scientific Flash 2000

https://doi.org/10.5194/egusphere-2026-2998
Preprint. Discussion started: 10 June 2026

elemental analyzer coupled to a Delta V isotope mass spectrometer. Inorganic carbon isotopes ($\delta^{13}C_{carb}$) were measured using the phosphoric acid reaction method on a GasBench system. All samples were analyzed in duplicate, with analytical precision of ± 0.2% for TOC and TN, and ± 0.2‰ for carbon isotopes (VPDB).

2.2 Organic matter extraction and separation of compound-grouped fractions

Surface sediments containing approximately 200 mg OC were ultrasonically extracted sequentially with *n*-hexane, dichloromethane, and a dichloromethane/methanol mixture (9:1, v/v). Prior to extraction, *n*-Tetracosane (*n*-$C_{24}D_{50}$) was added as an internal standard, and activated copper was used to remove elementary sulfur in sediments. The supernatants were combined and concentrated by evaporation.

The concentrated extracts were subjected to base hydrolysis using 1 M KOH in methanol at 70°C for 2 hours, followed by repeated extraction with *n*-hexane for recovery of neutral fractions. Hydrocarbon fractions containing aliphatics and aromatics were separated from neutral fractions using silica gel column chromatography by *n*-hexane/dichloromethane (7:3, v/v) as the eluent. The hydrocarbon fractions were further separated into straight chain alkanes (*n*-alkanes) and branched/cyclic alkanes via urea adduction for compound-specific stable carbon isotopic measurements, following the method of Xu & Sun (2005). C_{25} HBIs were present in the branched/cyclic fractions.

Lignin phenols were analyzed following the cupric oxide oxidation method (Hedges & Ertel, 1982; Goñi & Hedges, 1992; Hutchings et al., 2019). Briefly, sediment samples equivalent to approximately 10 mg OC were oxidized in 2N NaOH with 0.05 g of $Fe(NH_4)_2(SO_4)_2 \cdot 6H_2O$ and 0.5 g of CuO powder under N_2 gas at 170°C for 3 hours. The oxidation products were spiked with recovery standards (trans-cinnamic acid and ethyl vanillin), acidified to pH < 2 with 6N HCl, and kept in the dark for 1 h. After centrifugation, the products were subjected to liquid-liquid extraction with ethyl acetate and then concentrated under a stream of N_2 gas. The extracts were derivatized using *bis*-(trimethylsilyl)-trifluoroacetamide and trimethylchlorosilane (BSTFA+TMCS; 99:1) before gas chromatography analysis.

2.3 Molecular biomarker analysis

Hydrocarbon fractions containing *n*-alkanes, C_{25} HBIs, and terpenoids were analyzed with an Agilent 5977A mass spectrometry (MS) coupled to an Agilent 7890B gas chromatography (GC). The GC was equipped with a DB-1 MS capillary column (60 m × 0.32 mm × 0.25 μm). The oven temperature program was set as an initial temperature of 60°C for 2 min, then increased to 305°C at 4°C/min, and finally held at 305 °C for 35 minutes. Helium was used as the carrier gas with a flow rate of 1.0 mL/min. The transfer line temperature was 280°C, and the ion source temperature was 230 °C. The ion source was operated in electron impact (EI) mode at 70 eV, with full scan acquisition over m/z 50-650. Full scan was used to identify the biomarkers, and selected ion monitoring (SIM) for quantitative measurements of pentacyclic triterpenes (m/z = 191). In this study, several *n*-alkane indices were calculated to infer organic matter sources, including the carbon preference index (CPI; Silva et al., 2012), terrigenous-to-aquatic ratio (TAR; Silva et al., 2012), and aquatic plant index (P_{aq}; Mead et al., 2005).

https://doi.org/10.5194/egusphere-2026-2998
Preprint. Discussion started: 10 June 2026

The derivatized lignin phenols were analyzed using an Agilent 7890B gas chromatography equipped with a flame ionized detector (GC-FID). Chromatographic separation was achieved with a DB-1MS capillary column (60 m × 0.32 mm × 0.25 μm). The oven temperature was set at an initial 100°C for 2 min, then ramped to 270°C at 4°C/min, and held at 270°C for 15 min. Quantification of lignin phenols was based on a mixed lignin-derived phenol standard including syringaldehyde (SAL), acetosyringone (SON), syringic acid (SAD), vanillin (VAL), acetovanillone (VON), vanillic acid (VAD), *p*-coumaric acid (CAD), ferulic acid (FAD), *p*-hydroxybenzaldehyde (PAL), *p*-hydroxyacetophenone (PON), and *p*-hydroxybenzoic acid (PAD) (Fig S1).The eight major phenols, including syringyl (SAL, SON, SAD), vanillyl (VAL, VON, VAD), and cinnamyl (CAD, FAD) phenols, were normalized to the sample mass (Σ8, mg/10 g dry sediment). The cinnamyls to vanillyls ratio (C/V) was used to distinguish herbaceous from woody plants, and syringyls to vanillyls ratio (S/V) was used to distinguish gymnosperms from angiosperms (Tareq et al., 2004). The ratio of *p*-hydroxyl phenols to the sum of vanillyls and syringyls (P/(V+S)) was also calculated to assess the intensity of demethylation/demethoxylation reactions, usually with high values indicating greater demethylation/demethoxylation degradation (Dittmar & Lara, 2001).

2.4 Stable carbon isotope analysis of C_{25} HBIs

Stable carbon isotopic compositions of C_{25} HBIs were measured using a Thermo-Fisher Scientific Trace GC coupled with a MAT 253 isotope ratio mass spectrometry (IRMS). Chromatographic separation was achieved with a 60 m × 0.32 mm ID fused silica capillary column coated with a 0.25 μm film of DB-1 MS. Helium with a flow rate of 1.4 mL/min was used as the carrier gas. The GC oven temperature was initiated at 50 °C for 1 min, increased to 120°C at 15°C/min, then ramped to 305°C at 8°C/min, and finally held at 305°C for 21 min. The carbon isotope ratios of C_{25} HBIs were calibrated by reference gas with known $\delta^{13}C$ values (V-PDB standard). An external mixture of n-C_{16} to n-C_{30} with known $\delta^{13}C$ values from Indiana University, USA (B4 standard) was used to monitor the instrument performance. Normally, one injection of standards was performed for every three-sample injections. Samples analyzed in duplicate typically had an average standard deviation of ~ 0.5‰.

3 Results

3.1 Bulk characters of organic matter in surface sediments from Lake Haixihai

TOC values of surface sediments in Lake Haixihai range from 0.78% to 6.73% (Table 1). Generally, shallow water sediments have high TOC values (3.98% ± 1.56%) than deep water sediments (3.25% ± 0.69%). Carbonate contents (%$CaCO_3$) shows a similar pattern, with higher values in shallow water sediments (42.36% ± 16.54%) and lower values in deep water sediments (28.71% ± 9.25%). The $\delta^{13}C_{org}$ values exhibit a wide range, from -30.7‰ to -22.9‰. Shallow water sediments are relatively enriched in ^{13}C (−26.0‰ ± 1.6‰) compared to deep water sediments (-29.1‰ ± 1.3‰). In contrast, $\delta^{13}C_{carb}$ values show a narrower range, mainly between -5.2‰ and -0.7‰.

https://doi.org/10.5194/egusphere-2026-2998
Preprint. Discussion started: 10 June 2026

Table 1: Sampling information and bulk geochemical characters of organic matter in surface sediments of Lake Haixihai.

	Depth (m)	TOC (%)	TN (%)	TOC/TN	%$CaCO_3$	$\delta^{13}C_{org}$ (‰)	$\delta^{13}C_{carb}$ (‰)
S1	1.1	3.22	0.52	6.16	47.42	-22.9	-3.4
S2	5.2	4.02	0.38	10.55	39.82	-24.3	-3.3
S3	7.2	5.86	0.5	11.72	51.61	-25.2	-3.1
S4	5.2	0.78	0.12	6.67	24.73	-24.2	-3.3
S5	6.9	4.27	0.36	11.85	60.64	-26.4	-3.7
S6	8.3	2.69	0.22	12.52	25.88	-26.3	-1.4
S7	7.7	3.35	0.35	9.71	32.34	-24.8	-4.2
S8	10.9	3.46	0.35	9.91	37.36	-26.9	-3.4
S9	19.6	1.94	0.22	8.86	28.86	-27.0	-2.0
S10	9.8	4.81	0.49	9.73	32.50	-25.8	-5.2
S11	20	2.39	0.3	8.06	31.16	-28.3	-2.8
S12	9.7	2.55	0.19	13.28	88.04	-26.0	-0.7
S13	21.5	2.47	0.27	9.06	31.54	-27.6	-2.3
S14	10	3.91	0.38	10.27	37.58	-25.8	-3.6
S15	20.6	3.05	0.4	7.66	27.21	-29.4	-3.2
S16	22	2.97	0.34	8.87	19.40	-29.2	-3.5
S17	8.9	4.09	0.38	10.84	38.56	-26.0	-3.6
S18	9.8	4.87	0.4	12.07	38.77	-27.3	-3.9
S19	20.8	3.00	0.36	8.30	39.65	-29.3	-3.3
S20	19.8	3.43	0.38	9.14	26.09	-29.7	-3.7
S21	10.1	2.44	0.24	10.27	39.68	-27.0	-3.3
S22	9.9	6.60	0.53	12.55	46.88	-26.2	-4.1
S23	20.8	3.67	0.4	9.10	35.19	-29.7	-3.9
S24	20.4	3.64	0.44	8.31	2.87	-30.1	-3.8
S25	16	3.13	0.35	8.90	34.83	-28.9	-4.0
S26	21.1	3.18	0.39	8.08	21.24	-29.9	-3.6
S27	6.5	6.73	0.43	15.51	56.06	-25.4	-3.4
S28	19.8	3.23	0.40	8.16	31.58	-28.9	-3.6
S29	20.4	3.70	0.47	7.86	16.49	-30.1	-3.8
S30	20.1	4.44	0.51	8.75	25.87	-30.4	-3.9
S31	18.2	4.61	0.55	8.34	35.75	-30.7	-4.2
S32	19.90	3.78	0.46	8.21	32.08	-30.3	-4.3
S33	8.5	4.59	0.38	12.01	51.81	-26.6	-3.6
S34	8.3	3.10	0.36	8.54	20.60	-29.2	-3.4
S35	9.7	2.15	0.31	6.89	26.88	-29.0	-3.60

https://doi.org/10.5194/egusphere-2026-2998
Preprint. Discussion started: 10 June 2026

3.2 Molecular biomarkers in surface sediments of Lake Haixihai

3.2.1 *n*-Alkanes

n-Alkanes are dominated by mid- to long-chain homologues, with a pronounced odd-even carbon number predominance in the carbon range of nC_{23} to nC_{33} (Fig. 2). The carbon preference index (CPI) ranges from 3.53 to 7.26 (Table 2), typically indicative of land plant input to sedimentary organic matter. Most samples display a distinct unresolved complex mixture (UCM) in the nC_{23} – nC_{35} carbon range. However, deep water sediments contain relatively higher proportions of short- to mid-chain *n*-alkanes than shallow water sediments (Fig. 2), as indicated by higher nC_{21}-/nC_{22}+ ratios and the aquatic plant index (P_{aq}) (Table 2). P_{aq} ranges from 0.16 to 0.41, with higher values in deep water sediments (0.37 ± 0.04) than in shallow water sediments (0.30 ± 0.07). The terrigenous-to-aquatic ratio (TAR) varies between 1.14 and 12.01. It is higher in shallow water sediments (5.56 ± 2.84) and lower in deep water sediments (1.93 ± 0.92).

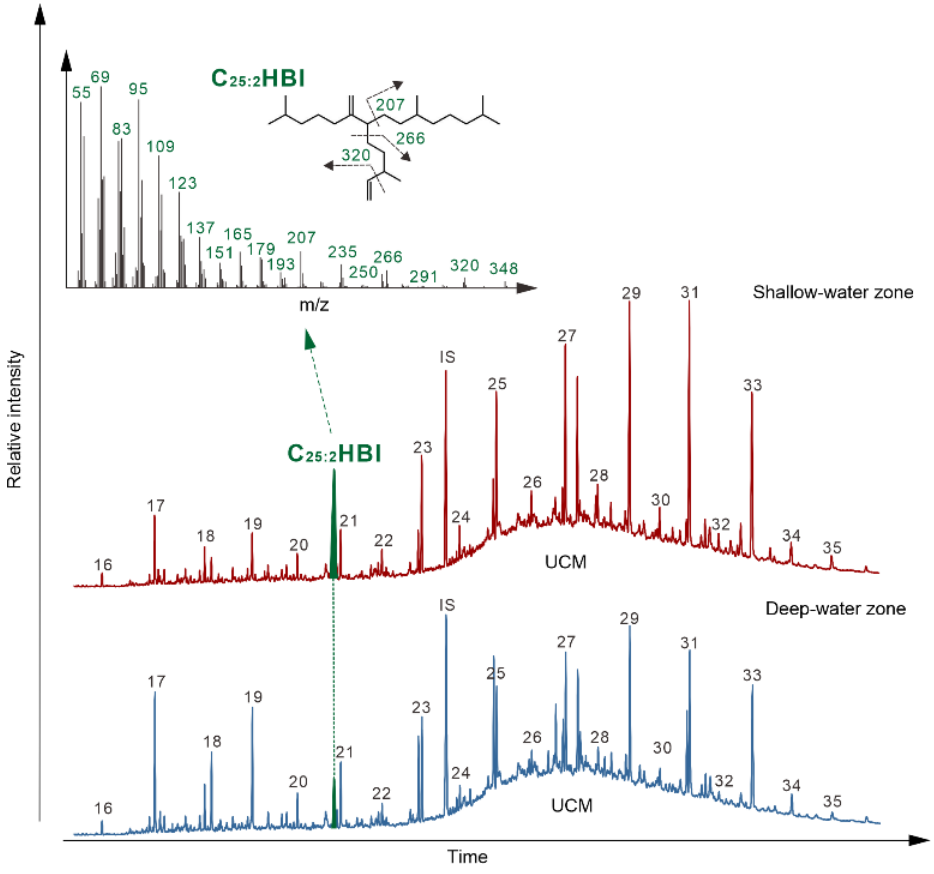

Figure 2: Total ion chromatogram of hydrocarbon fractions showing n-alkanes and $C_{25:2}$ HBIs distributions in surface sediments of Lake Haixihai. Mass spectral characteristics of $C_{25:2}$ HBIs and its structure are shown in the upper-left inset of the figure. Red chromatogram indicates typical shallow water samples (< 10 m) and blue chromatogram indicates typical deep water samples (> 10 m), respectively.

https://doi.org/10.5194/egusphere-2026-2998
Preprint. Discussion started: 10 June 2026

Table 2: Molecular parameters of organic matter in surface sediments of Lake Haixhai.

	CPI[a]	Paq[b]	TAR[c]	nC_{21}-/nC_{22}+[d]	$C_{25:2}$ HBI (ug/g dry sediment)	$C_{25:2}$ HBI (ug/g OC)	C_{30} ββ+Hopene[e] (ug/g OC)	Σ8[f] (mg/10 g dry sediment)	P/(S+V)[g]	$\delta^{13}C_{HBI}$ (‰)
S1	5.65	0.24	5.95	0.18	0.23	7.04	19.91	48.57	0.28	-
S2	7.26	0.21	8.38	0.15	0.30	7.43	21.21	40.99	0.36	-22.7
S3	5.23	0.30	3.61	0.27	1.13	19.36	35.36	34.62	0.40	-18.9
S4	6.37	0.27	9.60	0.16	0.01	1.83	6.74	1.11	0.28	-
S5	5.68	0.33	2.64	0.37	0.35	8.09	12.42	20.35	0.57	-
S6	6.16	0.27	6.31	0.22	0.16	6.06	9.76	18.30	0.17	-
S7	5.26	0.29	3.55	0.29	0.10	2.86	13.37	30.37	0.29	-
S8	7.13	0.39	4.27	0.25	0.27	7.87	28.02	17.06	0.42	-
S9	6.45	0.30	1.90	0.51	0.04	1.96	13.67	4.63	0.37	-
S10	6.05	0.16	12.01	0.13	0.06	1.26	15.30	33.79	0.23	-
S11	4.70	0.32	1.57	0.52	0.07	2.86	20.67	5.61	0.65	-
S12	5.87	0.24	7.31	0.18	0.05	2.01	5.44	15.05	0.20	-
S13	5.56	0.28	2.52	0.36	0.09	3.52	21.11	9.14	0.36	-
S14	5.31	0.35	5.42	0.21	0.39	9.99	26.10	29.39	0.44	-
S15	5.43	0.36	1.39	0.54	0.16	5.37	32.21	6.50	0.93	-
S16	4.59	0.40	1.15	0.64	0.20	6.86	29.35	5.70	0.98	-
S17	3.96	0.32	6.99	0.16	0.62	15.26	24.17	40.84	0.43	-19.7
S18	5.52	0.34	6.33	0.17	0.95	19.53	25.37	63.48	0.39	-20.6
S19	5.06	0.35	1.38	0.54	0.16	5.49	37.11	6.19	1.13	-
S20	5.48	0.35	1.66	0.47	0.26	7.59	33.41	8.41	1.05	-
S21	5.72	0.41	4.31	0.25	0.20	8.17	29.34	10.75	0.59	-
S22	4.66	0.41	5.98	0.17	1.30	19.69	23.51	98.09	0.46	-21.9
S23	5.31	0.37	1.62	0.48	0.28	7.67	36.58	10.33	1.07	-
S24	5.01	0.38	1.57	0.48	0.28	7.67	43.73	10.54	0.93	-
S25	4.98	0.36	1.89	0.45	0.35	11.32	34.63	9.79	0.60	-25.3
S26	5.06	0.40	1.18	0.61	0.18	5.70	31.53	8.69	0.94	-
S27	5.07	0.29	4.10	0.24	0.47	6.91	21.75	68.98	0.53	-20.9
S28	5.55	0.32	1.63	0.49	0.17	5.26	34.40	8.28	0.64	-24.5
S29	4.82	0.40	1.14	0.63	0.22	5.99	36.23	11.40	0.87	-
S30	5.33	0.39	1.78	0.44	0.39	8.69	43.06	18.17	0.82	-26.7
S31	4.02	0.41	1.78	0.43	0.48	10.46	47.93	21.36	0.76	-26.8
S32	4.71	0.39	2.08	0.40	0.36	9.50	37.30	15.62	0.77	-
S33	5.03	0.40	3.38	0.29	0.75	16.45	29.40	43.10	0.48	-20.7
S34	5.15	0.40	1.18	0.63	0.20	6.29	37.09	8.00	0.78	-
S35	3.53	0.37	1.85	0.44	0.10	4.45	18.98	7.91	0.37	-

https://doi.org/10.5194/egusphere-2026-2998
Preprint. Discussion started: 10 June 2026

[a] CPI = 1/2[$\Sigma(nC_{25\sim33})_{odd}/(nC_{24\sim32})_{even}+\Sigma(nC_{25\sim33})_{odd}/(nC_{26\sim34})_{even}$]
[b] $P_{aq} = (nC_{23+25})/(nC_{23+25+29+31})$
c TAR = $(nC_{27+29+31})/(nC_{15+17+19})$
[d] nC_{21}-/nC_{22}+ = $\Sigma(nC_{\leqslant21})/\Sigma(nC_{\geqslant22})$
[e] C_{30} ββ+Hopene = (C_{30} ββ-hopane)+(hop-17(21)-ene)+(hop-13(18)-ene)+diploptene.
[f] Σ8 = SAL+SON+SAD+VAL+VON+VAD+CAD+FAD
[g] P/(V+S) = (PAL+PON+PAD)/(VAL+VON+VAD+SAL+SON+SAD)

3.2.2 C_{25} highly branched isoprenoids (HBIs)

Identification of C_{25} HBIs was based on its mass spectra, retention time, and comparison with published reference spectra (Rowland & Robson, 1990; Johns et al., 1999; Belt et al., 2000; He et al., 2016; Behera et al., 2022). In the total ion chromatograms (TICs), the peak corresponding to the putative C_{25} HBIs elutes before nC_{21} on DB-1 MS capillary column (Fig. 2). The mass spectrum displays prominent fragment ions at m/z 207, 266, 320, and 348 (Fig. 2). This fragmentation pattern and retention time are consistent with those reported for $C_{25:2}$ HBI, with double bonds located at the C-6/C-17 and C-23/C-24 positions (Belt et al., 2000).

A highly abundant $C_{25:2}$ HBI was detected in surface sediments of Lake Haixihai, and its concentrations range from 0.01 to 1.30 μg/g dry sediment or from 1.26 to 19.69 μg/g OC (Table 2). In shallow water sediments, $C_{25:2}$ HBI concentrations range from 0.01 to 1.30 μg/g dry sediment or from 1.26 to 19.69 μg/g OC, with an average value of 0.42 ± 0.40 μg/g dry sediment or 9.09 ± 6.49 μg/g OC. In contrast, deep water sediments exhibit lower concentrations, ranging from 0.04 to 0.48 μg/g dry sediment or from 1.96 to 11.32 μg/g OC, with an average value of 0.23 ± 0.12 μg/g dry sediment or 6.77 ± 2.52 μg/g OC.

3.2.3 Hopanoids

The hopanoids in surface sediments of Lake Haixihai are dominated by 17β(H), 21β(H) (ββ) hopanes and hopenes, whereas17α(H), 21β(H) (αβ) and 17β(H), 21α(H) (βα) hopanes are less abundant (Fig. S2). The 17β(H)-hop-22(29)-ene (diploptene) is the most abundant compound across all samples, followed by hop-13(18)-ene, C_{30}ββ-hopane, C_{29}ββ-hopane, and C_{31}ββ-hopane. In this study, we designated ββ-hopane and hopenes as biological configured hopanoids and αβ- and βα-hopanes as geological configured hopanes (Peters et al., 2004; Sun et al., 2018). The combined concentrations of C_{30}ββ-hopane + hopenes range from 5.44 to 47.93 μg/g OC (Table 2). Deep water sediments have higher values (32.79 ± 8.48 μg/g OC) than shallow water sediments (20.35 ± 9.13 μg/g OC).

3.2.4 Lignin

Lignin abundances, indicated as Σ8, range from 1.11 to 98.09 mg/10 g dry sediment in surface sediments of Lake Haixihai (Table 2). Σ8 values are generally higher in shallow water sediments (35.47 ± 24.77 mg/10 g dry sediment) than those in deep water sediments (10.45 ± 4.71 mg/10 g dry sediment). The lignin degradation index, P/(S+V), varied between 0.17 and 1.13. Deep water sediments exhibit higher mean P/(S+V) values (0.77 ± 0.24) than shallow water sediments (0.39 ± 0.15).

https://doi.org/10.5194/egusphere-2026-2998
Preprint. Discussion started: 10 June 2026

3.3 Stable carbon isotopes of $C_{25:2}$ HBI

In this study, a total of 11 samples with relatively high $C_{25:2}$ HBI abundance were selected for separation and purification from hydrocarbon fractions, followed by compound-specific isotope analysis (Table 2). The stable carbon isotopic composition of $C_{25:2}$ HBI ($\delta^{13}C_{HBI}$) in these samples range from -26.8‰ to -18.9‰. The heaviest value is observed in sample S3 (-18.9‰), while the most ^{13}C-depleted value occurs in sample S31 (-26.8‰). The large variation in $\delta^{13}C_{HBI}$ among samples suggests strong spatial heterogeneity in the carbon isotopic composition.

4 Discussion

4.1 Sources of organic matter in surface sediments of Lake Haixihai

The availability of organic substrates controls microbial respiration and thus influences DIC composition (Bade et al., 2004; Karlsson et al., 2007; Sobek et al., 2009). This, in turn, affects the carbon isotopic signals recorded by primary producers given that these primary producers can use the respiration-derived DIC. The crossplot of $\delta^{13}C_{org}$ values and TOC/TN ratios has been widely used for a rough assessment of organic matter sources in modern sediments (Meyers, 1997). In Lake Haixihai, $\delta^{13}C_{org}$ values (-30.7‰ ~ -22.9‰) and TOC/TN ratios (6.16 ~ 12.55) indicate that shallow water sediments contain a mixture of algal and terrestrial organic matter, whereas deep water sediments are mainly dominated by algal input (Fig. 3a). The increasing contribution of terrestrial organic matter in the shallow area is evidenced by lower nC_{17} abundances (Fig. 2) and higher TAR ratios, which increase from 1.93 ± 0.92 in the deep area to 5.56 ± 2.84 in the shallow area. The nC_{17} is generally indicative of algal organic input into sediments (Peters et al., 2005). Whereas the TAR ratio, calculated from *n*-alkanes distributions, is widely applied to evaluate the relative contributions of terrestrial versus aquatic organic matter in modern sediments (Silva et al., 2012). However, the nC_{21}-/nC_{22}+ ratios (0.36 ± 0.16) suggest that both shallow and deep water sediments are dominated by terrestrial organic matter despite an increasing trend in this ratio from the shallow (0.25 ± 0.13) to the deep (0.47 ± 0.11) areas (Table 2). This is consistent with low phytoplankton biomass of oligotrophic Lake Haixihai (*Chl. a* concentration ~2.0 ug L^{-1}; Wang et al., 2019).

Although shallow water sediments receive substantial terrestrial input, lignin parameters (S/V vs. C/V) show that most terrestrial organic matter is derived from non-woody angiosperms, such as grasses and leaves (Fig. 3b; Tareq et al., 2004). Given the wide distribution of aquatic plants in nearshore areas (Fig. 1b), including *Potamogeton perfoliatus*, *Vallisneria natans*, *Myriophyllum spicatum L*, *Najas minor*, and *Utricularia*, these aquatic macrophytes likely contribute significantly to the terrestrial organic matter pool. The aquatic plant index (P_{aq}), an indicator reflecting the proportion of aquatic macrophytes based on the proportion of mid-chain to long-chain *n*-alkanes (Mead et al., 2005), is slightly higher in deep water sediments (0.37 ± 0.04) than in shallow water sediments (0.30 ± 0.07) (Table 2). This indicates that aquatic macrophytes and terrigenous inputs both contribute to sedimentary organic matter. Despite the small surface area of Lake Haixihai (3 km^2), nearshore sediments are strongly influenced by terrigenous input.

https://doi.org/10.5194/egusphere-2026-2998
Preprint. Discussion started: 10 June 2026

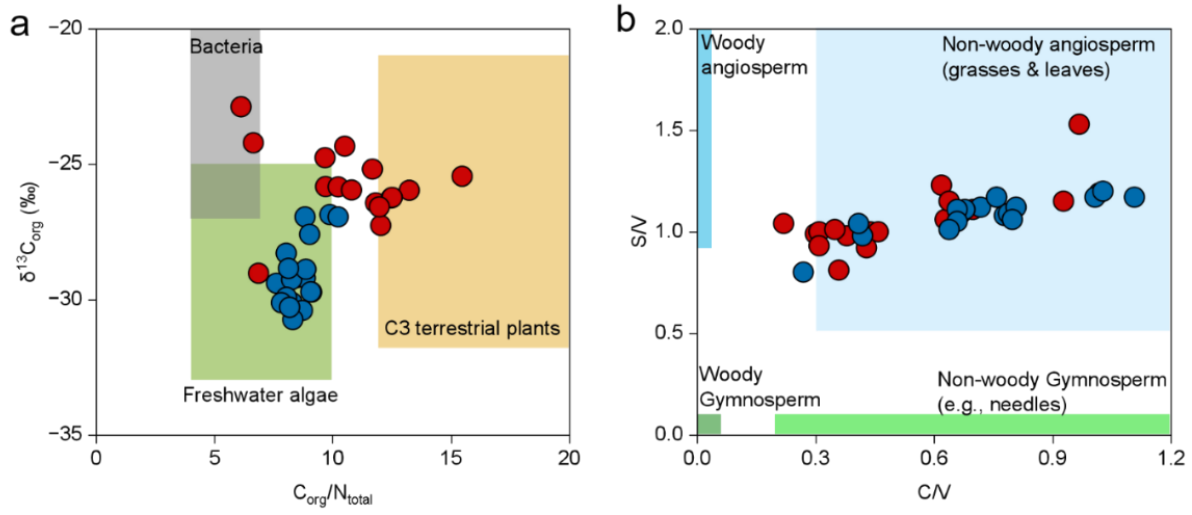

Figure 3: The δ^{13}Corg versus C/N ratio (a) and S/V versus C/V (b) of sedimentary organic matter in Lake Haixihai. Red symbols indicate shallow water samples (< 10 m) and blue symbols indicate deep water samples (> 10 m), respectively.

The distributions of hopanoids in the hydrocarbon fractions of surface sediments are dominated by biological configured ββ-hopane and hopenes, with minor contributions from geological configured αβ- and βα-hopanes (Fig. S2). This suggests strong microbial reworking of organic matter (López et al., 2015). Microbes biomass also contributes to the endogenous organic matter pool, as indicated by the prominent UCM hump in the TIC traces (Fig. 2; Silva et al., 2012; López et al., 2015).

Collectively, sedimentary organic matter in Lake Haixihai is mainly derived from aquatic macrophytes and terrigenous sources, with minor contributions from algae and bacterial input. Terrigenous input decreases from nearshore to deep water areas. This pattern is consistent with other macrophyte-dominated and oligotrophic lake systems (*e.g.*, Xiao et al., 2025).

4.2 Identification of microbial respiration-derived DIC utilized by diatoms in Lake Haixihai

Microbial respiration-derived DIC can be incorporated into $CaCO_3$ precipitation in lake systems (Sun et al., 2019). In deep water sediments of Lake Haixihai, $\delta^{13}C_{carb}$ exhibits a significant positive correlation with $\delta^{13}C_{org}$ (r = 0.748, p < 0.001; Fig. 4a) and a strong negative correlation with TOC (r = -0.852, p < 0.001; Fig. 4b). This indicates that carbonate precipitation is strongly influenced by respiration-derived DIC (Sun et al., 2019). By contrast, no significant correlation is observed in shallow water sediments between $\delta^{13}C_{carb}$ and $\delta^{13}C_{org}$ (r = 0.023, p > 0.05; Fig. 4a), and only a weak correlation exists with TOC (r = -0.378, p > 0.05; Fig. 4b). This likely reflects more complex carbon sources in nearshore settings, where both inorganic and organic carbon pools are more strongly influenced by lateral transport, sediment resuspension, and external inputs (Behera et al., 2022).

https://doi.org/10.5194/egusphere-2026-2998
Preprint. Discussion started: 10 June 2026

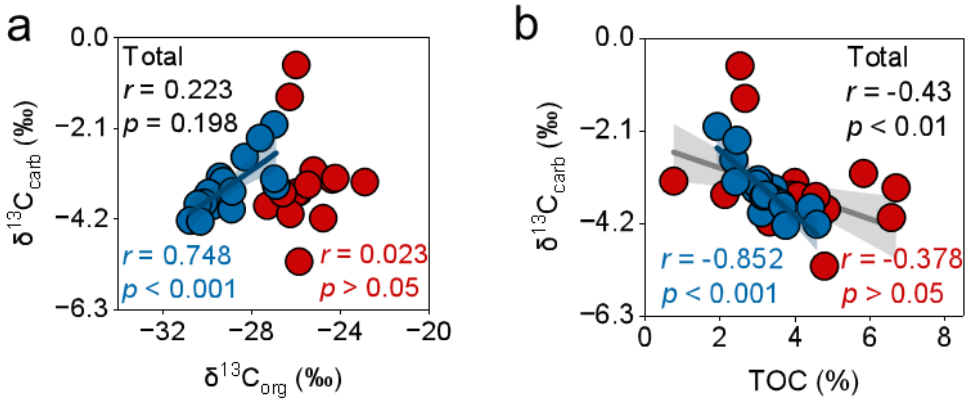

Figure 4: The relationship between $\delta^{13}C_{carb}$ and $\delta^{13}C_{org}$ (a) and TOC content (b). Red symbols indicate shallow water samples (< 10 m) and blue symbols indicate deep water samples (> 10 m), respectively.

In alkaline lakes, diatoms predominantly assimilate DIC from the water column. Hence, besides being sequestered via carbonate precipitation or released back to the atmosphere, respiration-derived DIC can serve as a potential source for diatom uptake, thus contributing to refixation within the biological carbon pump. As presented earlier, we successfully obtained $\delta^{13}C_{HBI}$ values for 11 samples. Two samples from northeastern Lake Haixihai (S2 and S3) occupy a particularly distinctive setting. As shown in the left-upper corner of Fig. 1b, they are located directly adjacent to a small marsh wetland. Their isotopic compositions may therefore be partly affected by biogeochemical processes in the marsh wetland. This two samples were thus excluded during the statistical analysis. The remaining samples show a strong positive correlation between $\delta^{13}C_{HBI}$ and $\delta^{13}C_{org}$ (r = 0.946, p < 0.001; Fig. 5a). Generally, this relationship can be readily interpreted as diatoms being the main contributor of organic matter. However, biomarker and geochemical evidence shows that organic matter in Lake Haixihai is mainly derived from aquatic macrophytes and terrestrial inputs, and minor from algae and bacteria inputs as discussed in Section 4.1. Thus, the synchronous isotopic variations reflect a close link between DIC utilized by diatoms and respiration-derived DIC within Lake Haixihai. If this interpretation is valid, $\delta^{13}C_{HBI}$ value should exhibit a dependence on the intensity of microbial reworking. Hopanoids in sediments are powerful tool for tracing microbial activity in surface environments (Peters et al., 2005; López et al., 2015; Sun et al., 2018). Enhanced microbial reworking of organic matter in surface environments is generally accompanied by elevated concentrations of biological configured hopanoids in surface sediments (Wu et al., 2025). In Lake Haixihai, concentrations of biological configured $C_{30}\beta\beta$-hopane + hopenes show a strong negative correlation with $\delta^{13}C_{HBI}$ (r = -0.92, p < 0.001; Fig. 5b), suggesting enhanced microbial reworking of organic matter within the water column and sediments and thereby substantially releasing ^{13}C-depleted DIC. This ^{13}C-depleted DIC can be further utilized by diatoms. Because DIC derived from microbial respiration is typically more depleted in ^{13}C than DIC supplied by carbonate dissolution and/or exchange with the atmosphere (Whiticar, 1999), utilization of this microbial respiration-derived DIC by diatoms can lead to ^{13}C-depleted isotopic compositions in C_{25} HBIs, as indicated by a negative correlation between concentrations of biological configured hopanoids and $\delta^{13}C_{HBI}$ values (Fig. 5b). Given that aquatic

https://doi.org/10.5194/egusphere-2026-2998
Preprint. Discussion started: 10 June 2026

macrophytes and terrigenous organic matter represent the dominant organic sources in the surface sediments of oligotrophic Lake Haixihai, the lignin distribution in these sediments provides further evidence showing that $\delta^{13}C_{HBI}$ values are strongly controlled by the intensity of microbial reworking of organic matter within the water column and sediments. The ratio P/(V+S) is employed to assess the intensity of demethylation/demethoxylation reactions, thereby reflecting the extent of organic matter degradation. High values typically indicate more extensive demethylation/demethoxylation (Dittmar & Lara, 2001). Similar to hopanoids, the P/(V+S) ratios is positively correlated with $\delta^{13}C_{HBI}$ (r = 0.93, p < 0.001; Fig. 5c), suggesting that microbial degradation controls the isotopic composition of DIC available to diatoms. It also indicates that aquatic macrophytes are an important substrate for microbial respiration in Lake Haixihai.

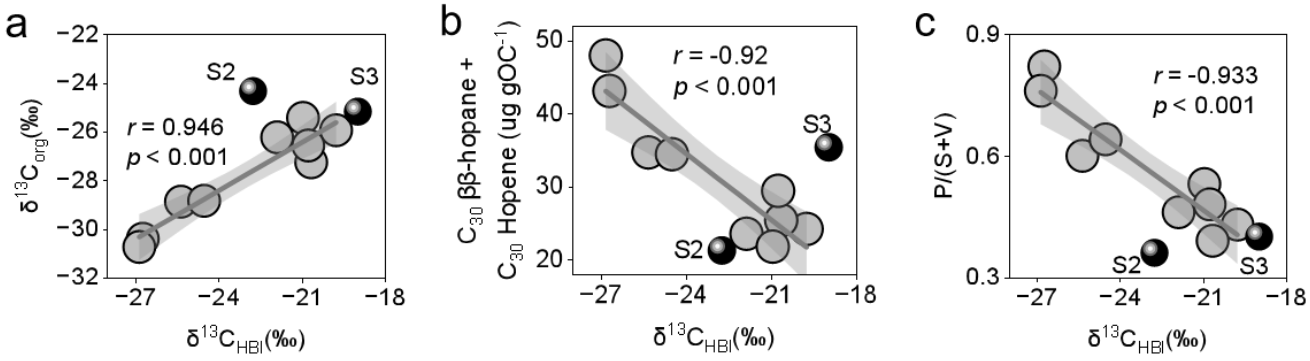

Figure 5: The relationship between $\delta^{13}C_{HBI}$ and $\delta^{13}C_{org}$ (a) and indicators of microbial respiration (b) and lignin degradation (c).

In Lake Haixihai, intense microbial activity helps maintain DIC pools enriched in respiration-derived carbon, as reflected by abundant biological configured hopanoids presented in extracted organic matter (Fig. S2). Concentrations of $C_{25:2}$ HBI are positively correlated with those of biological configured hopanoids in both shallow and deep water sediments (r = 0.65, p < 0.001 for shallow water, r = 0.74, p < 0.001 for deep water; Fig. 6a, b). $C_{25:2}$ HBI concentrations also increase with rising TOC (Fig. 6c, d). This observation suggests that higher OC contents provide more substrates for the production of respiration-derived DIC, which is then available for diatom growth. Meanwhile, continuous assimilation of respiration-derived DIC by diatoms promotes organic carbon production and burial. Although it is difficult at present to determine whether diatom abundance is controlled by substrate availability or environmental conditions (Karst-Riddoch et al., 2005), these strong positive relationships could be indicative of a corresponding diatom population that sustains the assimilating flux of respiration-derived DIC within lake systems.

https://doi.org/10.5194/egusphere-2026-2998
Preprint. Discussion started: 10 June 2026

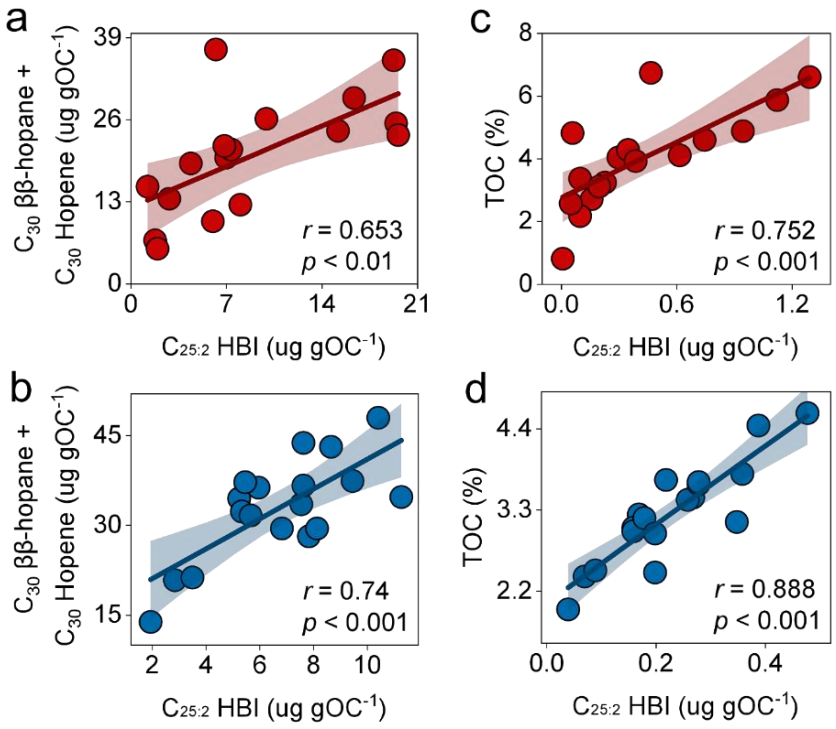

Figure 6: Relationships between diatom abundance ($C_{25:2}$ HBI) and indicators of microbial respiration (a and b) and TOC content (c and d). Red symbols indicate shallow water samples (< 10 m) and blue symbols indicate deep water samples (> 10 m), respectively.

4.3 Efficiency of diatoms in utilizing recycled carbon

The carbon mass-balance approach is a well-established tool for studying carbon cycling and quantifying carbon transformations in lake systems (Tranvik & Jansson, 2002; Leigh McCallister & del Giorgio, 2008). Compared to other phytoplankton groups such as cyanobacteria, diatoms are more sensitive to changes in DIC sources (Karst-Riddoch et al., 2005; Oduor & Schagerl, 2007; Shi et al., 2017). Consequently, diatoms respond more readily to variations in the fraction of respiration-derived DIC. This is evident in the $\delta^{13}C$ values of $C_{25:2}$ HBI in surface sediments of Lake Haixihai (Fig. 5). Here, we assume that diatoms utilize DIC from a mixture of recycled CO_2(aq) produced by microbial respiration and externally sourced DIC. The fraction of DIC from microbial respiration (f_{resp}) can be estimated using a two endmember mixing model:

$$\delta^{13}C_{utilized} = f_{resp} \cdot \delta^{13}C_{resp} + (1 - f_{resp}) \cdot \delta^{13}C_{ext} \quad (1)$$

Here, $\delta^{13}C_{utilized}$ is the isotopic composition of DIC assimilated by diatoms, $\delta^{13}C_{resp}$ is the isotopic signature of respiration-derived carbon, and $\delta^{13}C_{ext}$ is the isotopic value of externally sourced inorganic carbon.

External DIC in Lake Haixihai is mainly from carbonate weathering (0‰ - 2‰; Telmer & Veizer, 1999) and atmospheric CO_2 exchange (-8‰; Dubois et al., 2010). The local watershed $\delta^{13}C_{DIC}$ range (-4‰ to +1‰) was used to constrain this

https://doi.org/10.5194/egusphere-2026-2998
Preprint. Discussion started: 10 June 2026

endmember (Wang et al., 2019; Lai et al., 2024). The respiratory endmember ($\delta^{13}C_{resp}$) depends on organic matter in surface sediments of Lake Haixihai. Photodegradation and respiration in the water column were neglected due to very low dissolved organic carbon (DOC, ~0.5 mg/L) and particulate organic matter in Lake Haixihai, reflecting its oligotrophic state (low productivity with *Chl. a* = 2.0 ± 1.1 μg/L; Wang et al., 2019). Therefore, $\delta^{13}C_{resp}$ was estimated from sedimentary organic carbon ($\delta^{13}C_{org}$) with a 0.5‰ correction for microbial fractionation (Hullar et al., 1996; Karlsson et al., 2007). The $\delta^{13}C$ of DIC actually utilized by diatoms was calculated by $\delta^{13}C$ values of $C_{25:2}$ HBI:

$$\delta^{13}C_{utilized} = \delta^{13}C_{HBI} - \varepsilon_{photo} - \varepsilon_{b-l} \quad (2)$$

Here, ε_{photo} is the photosynthetic fractionation factor, reflecting carbon-concentrating mechanisms (CCMs) in diatoms under alkaline conditions (-12‰ to -6‰; Sharkey & Berry, 1985; Morales-Williams et al., 2017), and $\varepsilon_{b\text{-}l}$ is the lipid biosynthetic fractionation factor (3.7‰; Bouillon & Boschker, 2006; Leigh McCallister & del Giorgio, 2008). To ensure the accuracy of modeling results, uncertainties in all model parameters were propagated using Monte Carlo sensitivity analyses.

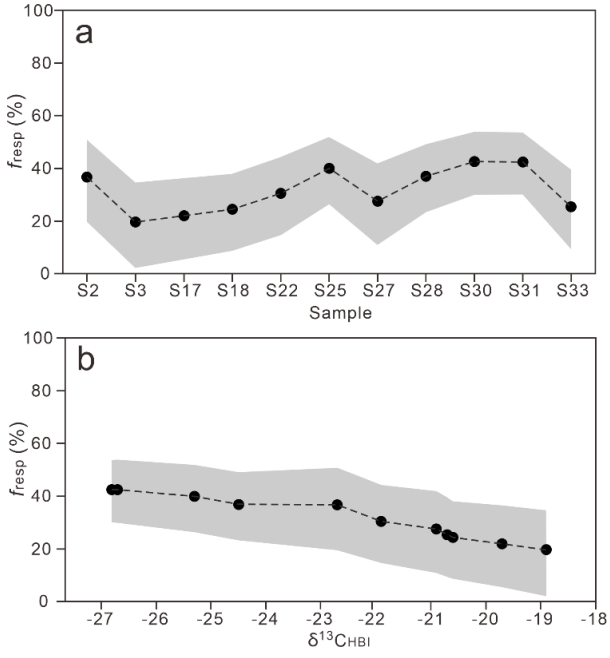

Figure 7: Estimated contribution of respired CO_2(aq) to diatom biosynthesis (f_{resp}) constrained by a two-endmember isotope mixing model. Results are based on Monte Carlo simulations that propagate uncertainty across all potential model parameters and presented respectively by sample number (a) and $\delta^{13}C_{HBI}$ (b). Dark black line represents median estimates and light black shading represents 95% uncertainty envelopes.

The modeling results indicate that respiration-derived DIC contributes about 31% ± 8% to diatom carbon uptake in Lake Haixihai (Fig. 7a). Surface sediments with ^{13}C-enriched C_{25} HBIs (approximately -22‰ to -19‰) exhibit lower f_{resp} values, with median estimates between 19% and 30% (Fig. 7b). In contrast, sediments containing strongly ^{13}C-depleted C_{25} HBIs (-27‰ to -23‰) have higher f_{resp}, ranging from 36% to 43%. The 95% confidence intervals mostly fall between 0% and 50%, indicating that recycled CO_2(aq) plays a significant role in diatom carbon uptake despite uncertainties (Fig. S3). This means

https://doi.org/10.5194/egusphere-2026-2998
Preprint. Discussion started: 10 June 2026

that diatoms efficiently utilize respiration-derived DIC, returning it to the biological carbon pump. This process likely account for the high organic carbon sequestration flux observed in Lake Haixihai despite its oligotrophic state (Wang et al., 2019). Combined with $CaCO_3$ precipitation, these pathways capture respired-derived DIC that would otherwise escape to the atmosphere, thereby enhancing internal carbon cycling and stabilizing carbon storage.

4.4 Implications for carbon cycling in aquatic systems

Alkaline lake systems commonly sustain stable diatom communities (Karst-Riddoch et al., 2005; Oduor & Schagerl, 2007; Duarte et al., 2008; Stenger-Kovács et al., 2014), and diatoms can utilize multiple forms of inorganic carbon across the water column (Tuite, 1981; Raven et al., 2011). Thus, the stable carbon isotopic composition of diatom-derived lipids is strongly influenced by the DIC pool composition (Corcoran et al., 2025). Our results reveal that CO_2(aq) released during microbial respiration of organic matter in alkaline lakes can be efficiently re-assimilated by diatoms through photosynthesis. This is particularly true for respiration-derived DIC, as this pattern is clearly reflected in the carbon isotopic records of C_{25} HBIs across diverse aquatic settings. Based on the compiled global $\delta^{13}C_{HBI}$ dataset from published literature (Fig. 8a), lake sediments exhibit lower $\delta^{13}C_{HBI}$ values (mean = -22‰, n = 23) than marine counterparts (mean = -16.6‰, n = 64), indicating a greater contribution of ^{13}C-depleted respiration-derived CO_2(aq) to diatom carbon uptake in lake systems (Fig. 8b). In open ocean settings, diatom growth mainly relies on CO_2(aq) that is continuously replenished via water-atmosphere exchange, resulting in relatively ^{13}C-enriched HBIs (Karlusich et al., 2021). As an endmember case, wetland systems show strongly ^{13}C-depleted HBIs (~ -39.3‰, n = 10), indicating a heavy dependence on recycled CO_2(aq). This pattern is likely driven by high organic loading, limited gas exchange, and active methane cycling (He et al., 2016). Hence, these observations suggest a gradient in carbon sources, with increasing reliance on recycled CO_2(aq) from marine to lake to wetland systems.

A very recent study by Diefendorf et al. (2025) found that C_{25} HBIs are widespread in lakes and can reach high concentrations (up to ~15.33 μg/g dry sediment). Many of these lakes are alkaline and contain large DIC pools (Stenger-Kovács et al., 2014; Diefendorf et al., 2025), supporting substantial diatom biomass capable of utilizing recycled CO_2(aq). Although our study focuses on diatoms, similar recycling pathways may also operate in other phytoplankton groups (Raven et al., 2011; Morales-Williams et al., 2017). Hence, a substantial fraction of respiration-derived DIC might be re-assimilated by these primary producers and subsequently reintroduced into the biological carbon pump. However, further study is needed to more accurately constrain both the efficiency and the flux of recycled CO_2(aq) fixation by diatoms. A key limitation is how to constrain the carbon isotopic composition of respiration-derived DIC. In Lake Haixihai, this uncertainty is relatively small due to its oligotrophic state and stable organic sources. However, ^{13}C-enriched DIC have been reported in eutrophic lakes, suggesting that carbon isotopic composition of the respiratory endmember may strongly depend on the dominant substrate type (*e.g.*, algae organic matter; Morales-Williams et al., 2017). Another source of uncertainty is photosynthetic fractionation. Our estimates likely represent a lower bound under strong CCMs activation. Enhanced CCM activity reduces photosynthetic carbon isotope fractionation, especially in alkaline lakes with low CO_2(aq). Under very low pCO_2 conditions, the ε_{photo} can decrease to -3‰ to -1‰, even to 0‰ (Sharkey & Berry, 1985; Erez et al., 1998). If these

https://doi.org/10.5194/egusphere-2026-2998
Preprint. Discussion started: 10 June 2026

reduced fractionations were applied, the inferred f_{resp} in our study would be higher. Also, improved endmember constraints and more robust treatment of multi-source mixing model will be essential for refining estimates of recycled carbon utilized by diatoms.

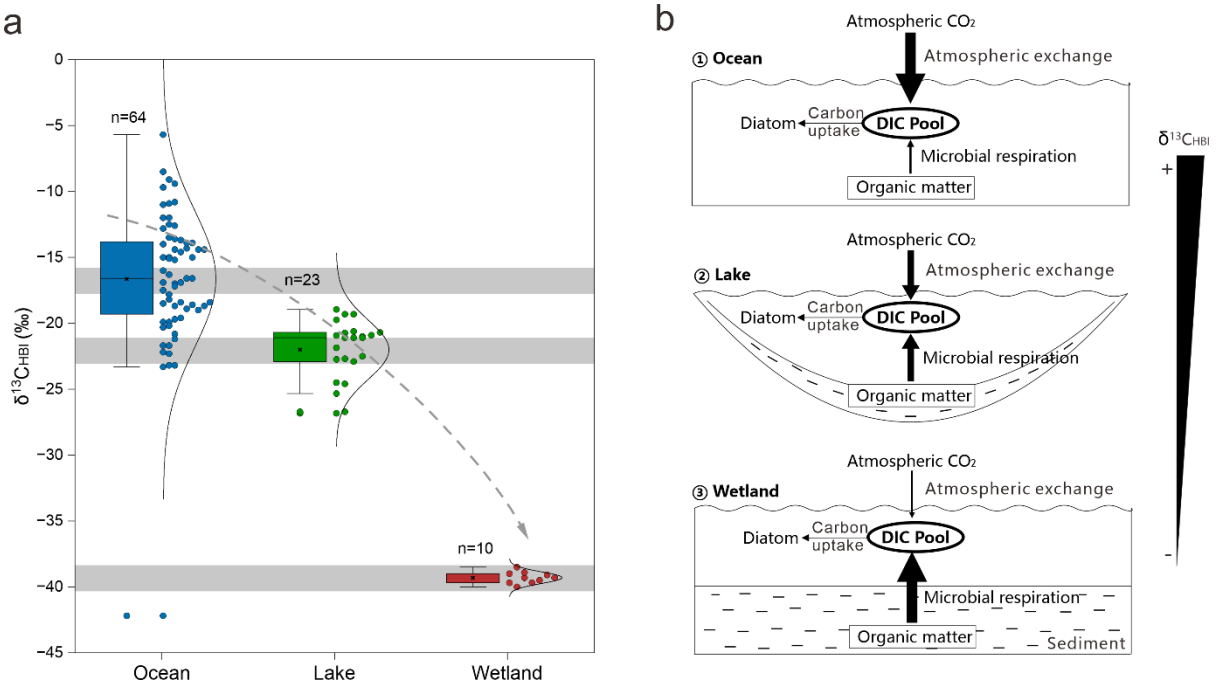

Figure 8: Systematic differences in $\delta^{13}C$ values of diatom-derived C_{25} HBIs among ocean, lake, and wetland. a, Boxplot comparison of $\delta^{13}C$ data for C_{25} HBIs from different aquatic systems. The carbon isotope dataset compiled here mainly includes $\delta^{13}C$ values of C_{25} HBIs compounds with zero to two double bonds. Detailed data and the corresponding references are provided in Fig. S4 and Table S1 of the Supplementary Materials. b, Conceptual diagram illustrating the relative proportions of atmospheric CO_2 exchange versus microbial respiration-derived inorganic carbon utilized by diatoms across ocean, lake, and wetland systems. Arrow thickness denotes the relative contribution of each carbon source to the dissolved inorganic carbon (DIC) pool. Atmospheric exchange decreases progressively from ocean to lake to wetland, whereas the contribution of microbial respiration of organic matter increases correspondingly. As a result, the $\delta^{13}C$ signature of the DIC pool available for diatom fixation becomes progressively more negative, which is recorded in the $\delta^{13}C$ values of diatom-derived C_{25} HBIs, showing a systematic depletion trend from ocean to lake to wetland.

Overall, the widespread occurrence of HBIs in lakes, the global variability in carbon isotopic signatures of C_{25} HBIs, and the quantitative constraints from the case of Lake Haixihai support a revised perspective on carbon cycling in inland waters. Lakes, particular alkaline lakes, should not be recognized easily as conduits for terrestrial carbon loss (Tranvik & Jansson, 2002). They are active systems in which biological re-fixation of respired carbon can substantially enhance long-term carbon sequestration and mitigate CO_2 emissions.

https://doi.org/10.5194/egusphere-2026-2998
Preprint. Discussion started: 10 June 2026

5 Conclusions

The carbon cycle in Lake Haixihai is characterized by a feedback loop in which CO_2(aq) released during microbial respiration is rapidly re-assimilated by diatoms. By linking degradation and fixation through a common DIC pool, the system maintains an efficient internal carbon turnover. This recycling pathway transforms respiration from a net carbon loss process into a contributor to primary production and sedimentary carbon sequestration. Extending beyond this system, such interactions point to a broader role of diatoms in mediating carbon turnover in inland waters, where recycled carbon may represent a key, yet underestimated, component of ecosystem carbon budgets.

Code and data availability

All raw data and supporting materials for this study are provided in the main text, figures, tables, and Supporting Information of this manuscript.

Author contributions

Dinggui Wu: Writing - review & editing, Writing - original draft, Visualization, Validation, Methodology, Investigation, Formal analysis, Data curation. Qingfeng Zhao: Resources, Investigation, Formal analysis. Siyu Huang: Writing - review & editing, Investigation. Yuxin He: Writing - review & editing, Supervision, Project administration, Investigation. Jinglu Wu: Writing - review & editing, Investigation. Yongge Sun: Writing - review & editing, Writing - original draft, Validation, Supervision, Project administration, Formal analysis, Conceptualization.

Competing interests

The authors declare there are no conflicts of interest for this manuscript.

Acknowledgements

This work was financially supported by the National Natural Science Foundation of China (42030803, 42073071).

References

Aichner, B., Wilkes, H., Herzschuh, U., Mischke, S., and Zhang, C.J. 2010: Biomarker and compound-specific $\delta^{13}C$ evidence for changing environmental conditions and carbon limitation at Lake Koucha, eastern Tibetan Plateau. J. Paleolimnol. 43: 873-899. https://doi.org/10.1007/s10933-009-9375-y.

https://doi.org/10.5194/egusphere-2026-2998
Preprint. Discussion started: 10 June 2026

Bade, D.L., Carpenter, S.R., Cole, J.J., Hanson, P.C., and Hesslein, R.H. 200: Controls of δ^{13}C-DIC in lakes: Geochemistry, lake metabolism, and morphometry. Limnol. Oceanogr. 49: 1160-1172. https://doi.org/https://doi.org/10.4319/lo.2004.49.4.1160.

Behera, D., Bhattacharya, S., Rahman, A., Kumar, S., and Anoop, A. 2022: Molecular tracers for characterization and distribution of organic matter in a freshwater lake system from the Lesser Himalaya. Biogeochemistry 161: 315-334. https://doi.org/10.1007/s10533-022-00984-y.

Belt, S.T., Allard, W.G., Massé, G., Robert, J.M., and Rowland, S.J. 2000: Highly branched isoprenoids (HBIs): Identification of the most common and abundant sedimentary isomers. Geochim. Cosmochim. Acta 64: 3839-3851. https://doi.org/10.1016/s0016-7037(00)00464-6.

Belt, S.T., Massé, G., Vare, L.L., Rowland, S.J., Poulin, M., Sicre, M.A., Sampei, M., and Fortier, L. 2008: Distinctive ^{13}C isotopic signature distinguishes a novel sea ice biomarker in Arctic sediments and sediment traps. Mar. Chem. 112: 158-167. https://doi.org/https://doi.org/10.1016/j.marchem.2008.09.002.

Belt, S.T., Smik, L., Brown, T.A., Kim, J.H., Rowland, S.J., Allen, C.S., Gal, J.K., Shin, K.H., Lee, J.I., and Taylor, K.W.R. 2016: Source identification and distribution reveals the potential of the geochemical Antarctic sea ice proxy IPSO25. Nat. Commun. 7: 12655. https://doi.org/10.1038/ncomms12655.

Bouillon, S., and Boschker, H.T.S. 2006: Bacterial carbon sources in coastal sediments: a cross-system analysis based on stable isotope data of biomarkers. Biogeosciences 3: 175-185. https://doi.org/10.5194/bg-3-175-2006.

Cole, J.J., Prairie, Y.T., Caraco, N.F., McDowell, W.H., Tranvik, L.J., Striegl, R.G., Duarte, C.M., Kortelainen, P., Downing, J.A., Middelburg, J.J., and Melack, J. 2007: Plumbing the Global Carbon Cycle: Integrating Inland Waters into the Terrestrial Carbon Budget. Ecosystems 10: 172-185. https://doi.org/10.1007/s10021-006-9013-8.

Corcoran, M.C., Diefendorf, A.F., Wiesenberg, N., Lowell, T.V., Wiles, G.C., Wilson, M.A., Bird, B.W., Naake, H., and Dietrich, W.L. 2025: Observed seasonal trends of diatom-derived C_{20} highly branched isoprenoids (HBIs): implications for paleoclimate studies. Geochim. Cosmochim. Acta 407: 211-223. https://doi.org/https://doi.org/10.1016/j.gca.2025.09.017.

Diefendorf, A.F., Dietrich, W.L., Naake, H., Corcoran, M.C., Kmetz, A.J., Lowell, T.V., Schenk, M.D., Wiles, G.C., and Wilson, M.A. 2025: Diatom-derived highly branched isoprenoids are diverse and widespread in lakes. Org. Geochem. 205: 104993. https://doi.org/https://doi.org/10.1016/j.orggeochem.2025.104993.

Dittmar, T., and Lara, R.J. 2001: Molecular evidence for lignin degradation in sulfate-reducing mangrove sediments (Amazônia, Brazil). Geochim. Cosmochim. Acta 65: 1417-1428. https://doi.org/https://doi.org/10.1016/S0016-7037(00)00619-0.

Dong, Y.X., Zhao, L., Jin, Y., Tang, X.Z., Zhou, Q.C., and Li, J. 2019: Research on algae in small natural plateau lakes with the area between 1 to 30 km^2 (in chinese). Environmental Science Survey 38: 16-23. https://doi.org/10.13623/j.cnki.hkdk.2019.01.006.

https://doi.org/10.5194/egusphere-2026-2998
Preprint. Discussion started: 10 June 2026

Duarte, C.M., Prairie, Y.T., Montes, C., Cole, J.J., Striegl, R., Melack, J., and Downing, J.A. 2008: CO_2 emissions from saline lakes: A global estimate of a surprisingly large flux. J. Geophys. Res.: Biogeosci. 113. https://doi.org/https://doi.org/10.1029/2007JG000637.

Dubois, K.D., Lee, D., and Veizer, J. 2010: Isotopic constraints on alkalinity, dissolved organic carbon, and atmospheric carbon dioxide fluxes in the Mississippi River. J. Geophys. Res.: Biogeosci. 115: 11. https://doi.org/10.1029/2009jg001102.

Erez, J., Bouevitch, A., and Kaplan, A. 1998: Carbon isotope fractionation by photosynthetic aquatic microorganisms: Experiments with Synechococcus PCC7942, and a simple carbon flux model. Canadian Journal of Botany 76: 1109-1118. https://doi.org/10.1139/b98-067.

Goñi, M.A., and Hedges, J.I. 1992: Lignin dimers: Structures, distribution, and potential geochemical applications. Geochim. Cosmochim. Acta 56: 4025-4043. https://doi.org/https://doi.org/10.1016/0016-7037(92)90014-A.

He, D., Simoneit, B.R.T., Xu, Y.P., and Jaffé, R. 2016: Occurrence of unsaturated C_{25} highly branched isoprenoids (HBIs) in a freshwater wetland. Org. Geochem. 93: 59-67. https://doi.org/10.1016/j.orggeochem.2016.01.006.

Hedges, J.I., and Ertel, J.R. 1982: Characterization of lignin by gas capillary chromatography of cupric oxide oxidation products. Anal. Chem. 54: 174-178. https://doi.org/10.1021/ac00239a007.

Hedges, J.I., Keil, R.G., and Benner, R. 1997: What happens to terrestrial organic matter in the ocean? Org. Geochem. 27: 195-212. https://doi.org/https://doi.org/10.1016/S0146-6380(97)00066-1.

Hullar, M., Fry, B., Peterson, B.J., and Wright, R.T. 1996: Microbial utilization of estuarine dissolved organic carbon: a stable isotope tracer approach tested by mass balance. Appl. Environ. Microbiol. 62: 2489-2493. https://doi.org/10.1128/aem.62.7.2489-2493.1996.

Hurrell, E.R., Barker, P.A., Leng, M.J., Vane, C.H., Wynn, P., Kendrick, C.P., Verschuren, D., and Alayne Street-Perrott, F. 2011: Developing a methodology for carbon isotope analysis of lacustrine diatoms. Rapid Commun. Mass Spectrom. 25: 1567-1574. https://doi.org/https://doi.org/10.1002/rcm.5020.

Hutchings, J.A., Bianchi, T.S., Kaufman, D.S., Kholodov, A.L., Vaughn, D.R., and Schuur, E.A.G. 2019: Millennial-scale carbon accumulation and molecular transformation in a permafrost core from Interior Alaska. Geochim. Cosmochim. Acta 253: 231-248. https://doi.org/10.1016/j.gca.2019.03.028.

Johns, L., Wraige, E.J., Belt, S.T., Lewis, C.A., Massé, G., Robert, J.M., and Rowland, S.J. 1999: Identification of a C_{25} highly branched isoprenoid (HBI) diene in Antarctic sediments, Antarctic sea-ice diatoms and cultured diatoms. Org. Geochem. 30: 1471-1475. https://doi.org/https://doi.org/10.1016/S0146-6380(99)00112-6.

Kaiser, J., Belt, S.T., Tomczak, M., Brown, T.A., Wasmund, N., and Arz, H.W. 2016: C_{25} highly branched isoprenoid alkenes in the Baltic Sea produced by the marine planktonic diatom *Pseudosolenia calcar-avis*. Org. Geochem. 93: 51-58. https://doi.org/10.1016/j.orggeochem.2016.01.002.

Karlsson, J., Jansson, M., and Jonsson, A. 2007: Respiration of allochthonous organic carbon in unproductive forest lakes determined by the Keeling plot method. Limnol. Oceanogr. 52: 603-608. https://doi.org/https://doi.org/10.4319/lo.2007.52.2.0603.

https://doi.org/10.5194/egusphere-2026-2998
Preprint. Discussion started: 10 June 2026

Karlusich, J.J.P., Bowler, C., and Biswas, H. 2021: Carbon dioxide concentration mechanisms in natural populations of marine diatoms: Insights from Tara oceans. Front. Plant Sci. 12: 19. https://doi.org/10.3389/fpls.2021.657821.

Karst-Riddoch, T.L., Pisaric, M.F.J., and Smol, J.P. 2005: Diatom responses to 20th century climate-related environmental changes in high-elevation mountain lakes of the northern Canadian Cordillera. J. Paleolimnol. 33: 265-282. https://doi.org/10.1007/s10933-004-5334-9.

Lai, C., Liu, Z., Yu, Q., Sun, H., Xia, F., He, X., Ma, Z., Han, Y., Liu, X., Hao, P., Bao, Q., Shao, M., and He, H. 2024: Control of carbon dioxide exchange fluxes by rainfall and biological carbon pump in karst river–lake systems. Sci. Total Environ. 937: 173486. https://doi.org/https://doi.org/10.1016/j.scitotenv.2024.173486.

Leigh McCallister, S., and del Giorgio, P.A. 2008: Direct measurement of the $d^{13}C$ signature of carbon respired by bacteria in lakes: Linkages to potential carbon sources, ecosystem baseline metabolism, and CO_2 fluxes. Limnol. Oceanogr. 53: 1204-1216. https://doi.org/https://doi.org/10.4319/lo.2008.53.4.1204.

Liu, Z. 2023. DIC fertilization of primary production in karst lake-reservoirs and its effects on carbon sequestration and mitigation of eutrophication. Chin. Sci. Bull. 68: 915-926.

López, L., Lo Mónaco, S., and Volkman, J.K. 2015: Evidence for mixed and biodegraded crude oils in the Socororo field, Eastern Venezuela Basin. Org. Geochem. 82: 12-21. https://doi.org/https://doi.org/10.1016/j.orggeochem.2015.02.006.

Mead, R., Xu, Y., Chong, J., and Jaffé, R. 2005: Sediment and soil organic matter source assessment as revealed by the molecular distribution and carbon isotopic composition of n-alkanes. Org. Geochem. 36: 363-370. https://doi.org/https://doi.org/10.1016/j.orggeochem.2004.10.003.

Meyers, P.A., and Ishiwatari, R. 1993: Lacustrine organic geochemistry-an overview of indicators of organic matter sources and diagenesis in lake sediments. Org. Geochem. 20: 867-900. https://doi.org/https://doi.org/10.1016/0146-6380(93)90100-P.

Morales-Williams, A.M., Wanamaker Jr, A.D., and Downing, J.A. 2017: Cyanobacterial carbon concentrating mechanisms facilitate sustained CO_2 depletion in eutrophic lakes. Biogeosciences 14: 2865-2875. https://doi.org/10.5194/bg-14-2865-2017.

Oduor, S.O., and Schagerl, M. 2007: Phytoplankton primary productivity characteristics in response to photosynthetically active radiation in three Kenyan Rift Valley saline–alkaline lakes. J. Plankton Res. 29: 1041-1050. https://doi.org/10.1093/plankt/fbm078.

Peters, K.E., Walters, C.C., and Moldowan, J.M. 2004: Book Organic chemistry. Peters, K.E., Walters, C.C..Moldowan, J.M. (eds), pp. 18-44, Cambridge University Press, Cambridge.

Pietzsch, R. 2026: A global assessment of the geochemistry of carbonate mineral formation and the dynamics of calcite precipitation in alkaline lakes. Earth Sci. Rev. 272: 105347. https://doi.org/https://doi.org/10.1016/j.earscirev.2025.105347.

Raven, J.A., Giordano, M., Beardall, J., and Maberly, S.C. 2011: Algal and aquatic plant carbon concentrating mechanisms in relation to environmental change. Photosynth. Res. 109: 281-296. https://doi.org/10.1007/s11120-011-9632-6.

Raven, J.A., and Waite, A.M. 2004: The evolution of silicification in diatoms: inescapable sinking and sinking as escape? New Phytol. 162: 45-61. https://doi.org/https://doi.org/10.1111/j.1469-8137.2004.01022.x.

https://doi.org/10.5194/egusphere-2026-2998
Preprint. Discussion started: 10 June 2026

Rowland, S.J., and Robson, J.N. 1990: The widespread occurrence of highly branched acyclic C-20, C-25 and C-30 hydrocarbons in recent sediments and biota - A review. Marine Environmental Research 30: 191-216. https://doi.org/10.1016/0141-1136(90)90019-k.

Sharkey, T.D., and Berry, J.A. 1985: Carbon isotope fractionation of algae as influenced by an inducible CO_2 concentrating mechanism, American Society of Plant Physiologists, Rockville.

Shi, X., Li, S., Wei, L., Qin, B., and Brookes, J.D. 2017: CO_2 alters community composition of freshwater phytoplankton: A microcosm experiment. Sci. Total Environ. 607-608: 69-77. https://doi.org/https://doi.org/10.1016/j.scitotenv.2017.06.224.

Silva, T.R., Lopes, S.R.P., Spörl, G., Knoppers, B.A., and Azevedo, D.A. 2012: Source characterization using molecular distribution and stable carbon isotopic composition of n-alkanes in sediment cores from the tropical Mundaú–Manguaba estuarine–lagoon system, Brazil. Org. Geochem. 53: 25-33. https://doi.org/https://doi.org/10.1016/j.orggeochem.2012.05.009.

Sobek, S., Durisch-Kaiser, E., Zurbrügg, R., Wongfun, N., Wessels, M., Pasche, N., and Wehrli, B. 2009: Organic carbon burial efficiency in lake sediments controlled by oxygen exposure time and sediment source. Limnol. Oceanogr. 54: 2243-2254. https://doi.org/https://doi.org/10.4319/lo.2009.54.6.2243.

Stenger-Kovács, C., Lengyel, E., Buczkó, K., Tóth, F.M., Crossetti, L.O., Pellinger, A., Doma, Z.Z., and Padisák, J. 2014: Vanishing world: alkaline, saline lakes in Central Europe and their diatom assemblages. Inland Waters 4: 383-396. https://doi.org/10.5268/iw-4.4.722.

Striegl, R.G., Kortelainen, P., Chanton, J.P., Wickland, K.P., Bugna, G.C., and Rantakari, M. 2001: Carbon dioxide partial pressure and ^{13}C content of north temperate and boreal lakes at spring ice melt. Limnol. Oceanogr. 46: 941-945. https://doi.org/https://doi.org/10.4319/lo.2001.46.4.0941.

Summons, R.E., Barrow, R.A., Capon, R.J., Hope, J.M., and Stranger, C. 1993: The structure of a new C_{25} isoprenoid alkene biomarker from diatomaceous microbial communities. Aust. J. Chem. 46: 907-915. https://doi.org/10.1071/ch9930907.

Sun, D., He, Y., Wu, J., Liu, W., and Sun, Y. 2019: Hydrological and ecological controls on autochthonous carbonate deposition in lake systems: A case study from lake wuliangsu and the global perspective. Geophys. Res. Lett. 46: 6583-6593. https://doi.org/https://doi.org/10.1029/2019GL082224.

Sun, D., Tang, J., He, Y., Liao, W., and Sun, Y. 2018: Sources, distributions, and burial efficiency of terrigenous organic matter in surface sediments from the Yellow River mouth, northeast China. Org. Geochem. 118: 89-102. https://doi.org/https://doi.org/10.1016/j.orggeochem.2017.12.009.

Tareq, S.M., Tanaka, N., and Ohta, K. 2004: Biomarker signature in tropical wetland: lignin phenol vegetation index (LPVI) and its implications for reconstructing the paleoenvironment. Sci. Total Environ. 324: 91-103. https://doi.org/https://doi.org/10.1016/j.scitotenv.2003.10.020.

Telmer, K., and Veizer, J. 1999: Carbon fluxes, pCO_2 and substrate weathering in a large northern river basin, Canada: carbon isotope perspectives. Chem. Geol. 159: 61-86. https://doi.org/https://doi.org/10.1016/S0009-2541(99)00034-0.

Tranvik, L.J., Downing, J.A., Cotner, J.B., Loiselle, S.A., Striegl, R.G., Ballatore, T.J., Dillon, P., Finlay, K., Fortino, K., Knoll, L.B., Kortelainen, P.L., Kutser, T., Larsen, S., Laurion, I., Leech, D.M., McCallister, S.L., McKnight, D.M., Melack,

https://doi.org/10.5194/egusphere-2026-2998
Preprint. Discussion started: 10 June 2026

J.M., Overholt, E., Porter, J.A., Prairie, Y., Renwick, W.H., Roland, F., Sherman, B.S., Schindler, D.W., Sobek, S., Tremblay, A., Vanni, M.J., Verschoor, A.M., von Wachenfeldt, E., and Weyhenmeyer, G.A. 2009: Lakes and reservoirs as regulators of carbon cycling and climate. Limnol. Oceanogr. 54: 2298-2314. https://doi.org/https://doi.org/10.4319/lo.2009.54.6_part_2.2298.

Tranvik, L.J., and Jansson, M. 2002: Terrestrial export of organic carbon. Nature 415: 861-862. https://doi.org/10.1038/415861b.

Tuite, C.H. 1981: Standing crop densities and distribution of Spirulina and benthic diatoms in East African alkaline saline lakes. Freshwater Biol. 11: 345-360. https://doi.org/https://doi.org/10.1111/j.1365-2427.1981.tb01266.x.

Vuorio, K., Meili, M., and Sarvala, J. 2006: Taxon-specific variation in the stable isotopic signatures ($\delta^{13}C$ and $\delta^{15}N$) of lake phytoplankton. Freshwater Biol. 51: 807-822. https://doi.org/10.1111/j.1365-2427.2006.01529.x.

WABD. 2012: Water Conservancy History of Dali Bai Autonomous Prefecture. Yunnan Science and Technology Press (in chinese).

Wang, J.Y., Chen, G.J., Kang, W.G., Hu, K., and Wang, L. 2019: Impoundment intensity determines temporal patterns of hydrological fluctuation, carbon cycling and algal succession in a dammed lake of Southwest China. Water Res. 148: 162-175. https://doi.org/10.1016/j.watres.2018.10.032.

Webb, M., Barker, P.A., Wynn, P.M., Heiri, O., van Hardenbroek, M., Pick, F., Russell, J.M., Stott, A.W., and Leng, M.J. 2016: Interpretation and application of carbon isotope ratios in freshwater diatom silica. J. Quat. Sci. 31: 300-309. https://doi.org/10.1002/jqs.2837.

Whiticar, M.J. 1999: Carbon and hydrogen isotope systematics of bacterial formation and oxidation of methane. Chem. Geol. 161: 291-314. https://doi.org/https://doi.org/10.1016/S0009-2541(99)00092-3.

Wu, M., Wang, X., He, K., Su, J., and Zhang, S. 2025: Biomarker proxies for redox-controlled biodegradation: Deciphering organic matter preservation and carbon cycling. Geochim. Cosmochim. Acta 405: 148-161. https://doi.org/https://doi.org/10.1016/j.gca.2025.07.030.

Xiao, B., Cheecham-Uhrich, D., Eickmeyer, D.C., Kimpe, L.E., Prėskienis, V., Henriikka Kivilä, E., Man, M., Simpson, M.J., Creed, I., Rautio, M., and Blais, J.M. 2025: Long chain n-alkanes in lake sediment track differences in adjacent land vegetation. Org. Geochem. 202: 104934. https://doi.org/https://doi.org/10.1016/j.orggeochem.2025.104934.

Xu, S., and Sun, Y. 2005: An improved method for the micro-separation of straight chain and branched/cyclic alkanes: Urea inclusion paper layer chromatography. Org. Geochem. 36: 1334-1338. https://doi.org/https://doi.org/10.1016/j.orggeochem.2005.04.003.

Zhang, Y.D., Su, Y.L., Liu, Z.W., Kong, L.Y., Yu, J.L., and Jin, M. 2018: Aliphatic hydrocarbon biomarkers as indicators of organic matter source and composition in surface sediments from shallow lakes along the lower Yangtze River, Eastern China. Org. Geochem. 122: 29-40. https://doi.org/10.1016/j.orggeochem.2018.04.009.